JOURNAL OF COLLOID AND INTERFACE SCIENCE **189,** 236–241 (1997)
ARTICLE NO. CS974828

Static Light Scattering Study of Size Parameters in Core–Shell Colloidal Systems

Arturo Quirantes,[1] Rosario Plaza, and Angel Delgado

Departamento de Física Aplicada, Facultad de Ciencias, Universidad de Granada, 18071 Granada, Spain

Received July 22, 1996; accepted February 17, 1997

The applicability of static light scattering as a tool for particle sizing is evaluated for spherical core–shell systems. A series of intensity–angle measurements have been made on hematite (α-Fe_2O_3) particles covered by yttrium basic carbonate ($Y(OH)CO_3$) shells; size parameters—including polydispersity—have been deduced by means of the Aden–Kerker scattering theory, and the results have been compared to electron microscopy. Some explanations are given concerning the higher degree of polydispersity yielded by Aden–Kerker theory compared to electron microscopy observations.

Key Words: **light scattering; coated spheres; size parameters.**

INTRODUCTION

Light scattering has traditionally been used to obtain information about particles in colloidal suspensions. As a nonintrusive and nondestructive method with many applications, it is especially useful to probe systems *in situ* and in real time, thereby providing information about particle size, shape, composition, structure, and orientation. Many applications of the subject are based on solving the so-called inverse problem: given the electric field scattered by a system, describe the particle (or particles) responsible for the scattering.

Real applications of the inverse-problem approach to particle sizing require the assumption of a given shape, so that Maxwell's equations can be adequately solved. Light scattering by spherical particles was studied by Mie (1) and, although his theory is subject to some constraints (e.g., particle homogeneity), it has typically been applied to most light scattering experiments, often beyond those which are theoretically justified. In the recent past, many theories have been developed that yield a more accurate description of light scattering in non-Mie situations (e.g., nonspherical, nonhomogeneous, aggregated systems). One of the first of such theoretical developments concerned mono- and multicoated spheres.

Presently, static light scattering is used to determine the size (or size distribution) of core–shell systems of biological and biochemical significances, ranging from vesicles and microemulsions to polymers (2–6). Pharmaceutical applications include the study of coated particles as potential delivery systems.

In this work, light scattering has been applied to the study of hematite (α-Fe_2O_3) core particles surrounded by an yttrium basic carbonate ($Y(OH)CO_3$) coating. The techniques for their synthesis allow the preparation of a wide range of shell thicknesses. These methods permitted testing of the applicability and limitations of static light scattering sizing techniques in different situations, including cases where the particles were moderately polydisperse. The system described in this work is also of a practical interest: it is a first step in the synthesis of hematite particles coated with yttrium oxide shells, which are known to have many applications in superconductivity research. It is expected that light scattering analysis will determine the dimensions of both the nucleus and the coated shell, so that the physical characteristics of a colloidal system synthesized under similar conditions can be evaluated without the use of microphotography throughout the entire synthesis process.

THEORY

In the present work, Aden and Kerker's (7) scattering theory for concentric spherical particles has been used. The geometry of the system is shown in Fig. 1. A spherical, coated particle of inner radius X, outer radius Y, and coat thickness $Z(Y - X)$ is illuminated by a monochromatic radiation beam of wavelength λ_0 (the (complex) refractive indices of the core, shell, and suspending medium are n_1, n_2, and n_0, respectively). For incident radiation that is polarized perpendicularly to the scattering plane (defined by the incident and observation directions), the theory for concentric spherical particles by Aden and Kerker (7) yields the intensity $i(\theta)$ scattered by a single particle at an angle θ in the form

$$i(\theta) = I_0 \frac{\lambda_0^2}{4\pi^2 r^2} |S_1(\theta)|^2, \quad [1]$$

[1] To whom correspondence should be addressed. E-mail: aquiran@goliat.ugr.es.

0021-9797/97 $25.00

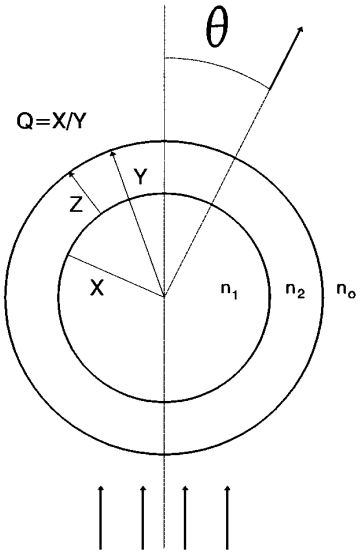

FIG. 1. Geometry of the scattering system.

where r is the distance between the particle and the observer, I_0 is the intensity of the incident radiation, and $S_1(\theta)$ is an infinite series of the form

$$S_1(\theta) = \sum_{n=1}^{\infty} \frac{2n+1}{n(n+1)} [a_n \pi_n(\theta) + b_n \tau_n(\theta)]. \quad [2]$$

The amplitudes a_n and b_n are functions of:

—the size parameters $x = kX$ and $y = kY$, where $k = 2\pi/\lambda = 2\pi n_0/\lambda_0$;

—the relative refractive indices $m_1 = n_1/n_0$ and $m_2 = n_2/n_0$

(see Appendix). The angular functions $\pi_n(\theta)$ and $\tau_n(\theta)$ are related to the associated Legendre functions $P_n^1(\theta)$ (8) as

$$\pi_n(\theta) = \frac{P_n^1(\theta)}{\text{sen } \theta} \qquad \tau_n(\theta) = \frac{dP_n^1(\theta)}{d\theta}. \quad [3]$$

In the absence of multiple scattering, the intensity of light scattered by a system of N identical monodisperse particles is simply $Ni(\theta)$. Since real systems are rarely monodisperse, a size distribution $p(d)$ must be allowed for, accounting for a distribution of dimensions in both the core and the shell:

$$i(\theta) = \int_0^{\infty} \int_0^{\infty} i(\theta, X, Y) p(X) p(Y) dX dY. \quad [4]$$

In our calculations, we used a Zeroth-Order Logarithmic Distribution (ZOLD) (9),

$$p(d) = \frac{1}{\sqrt{2\pi}\, d_m \sigma_0 e^{\sigma_0^2/2}} \exp\left[- \frac{(\ln d - \ln d_m)^2}{2\sigma_0^2} \right], \quad [5]$$

which is characterized by its modal diameter (d_m) and width (σ_0). In the general case, seven parameters were needed to calculate $i(\theta)$: three refractive indices and two size parameters (modal diameter and width) for both the core and the shell. This number would increase to ten if we consider fully complex refractive indices, where the imaginary part accounts for absorption of the incident radiation.

MATERIALS AND METHODS

Particle synthesis was carried out as described in (10–12). The core hematite particles (Fig. 2) were produced by the homogeneous precipitation method of Matijević and Scheiner (10): a 0.018 M $FeCl_3$ (Merck) + 0.001 M HCl (Merck) solution was heated at 100°C for 24 h. The resulting dispersion was repeatedly cleaned by centrifugation and redispersion in doubly distilled, deionized water (Milli-Q,

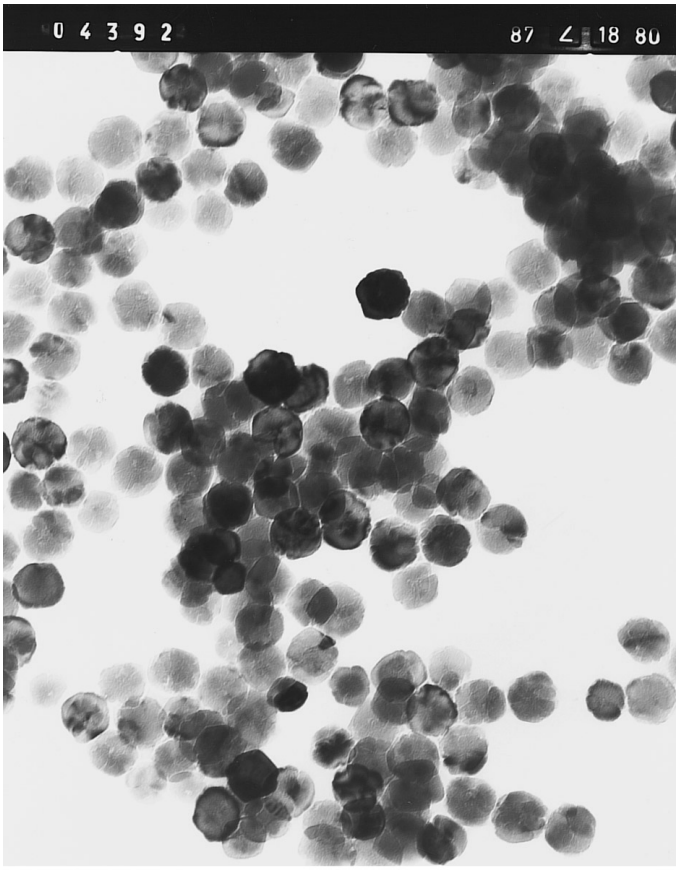

FIG. 2. TEM picture of the hematite core particles. Bar length, 100 nm.

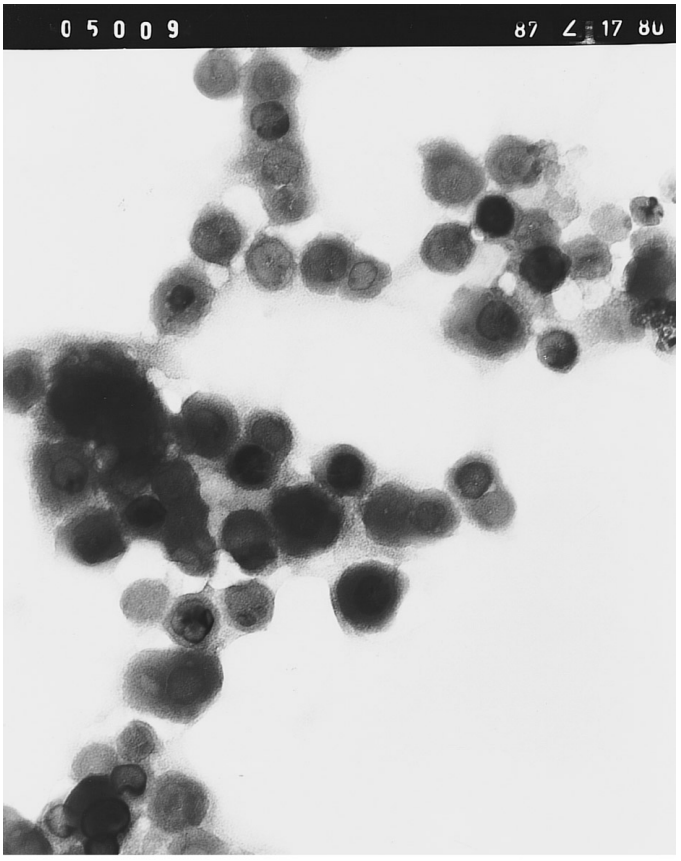

FIG. 3. TEM pictures of coated particles, sample B_9. Bar length, 100 nm.

Millipore), treated with 1 *M* NaOH and further cleaned by serum replacement.

The yttrium basic carbonate coating was obtained (11, 12) by heating to 90°C aqueous suspensions containing 6.5×10^{-4} *M* hematite and different concentrations of $Y(NO_3)_3$ (Merck). The thickness of the shell was controlled by varying the aging time and the initial yttrium nitrate concentration. In the three coated samples described in this work we varied the shell thickness, obtaining samples named B_2 (2 h aging, $[Y(NO_3)_3] = 0.003$ *M*), B_9 (9 h aging, $[Y(NO_3)_3] = 0.003$ *M*), and D_9 (9 h aging, $[Y(NO_3)_3] = 0.001$ *M*). Figure 3 shows a TEM picture of one of the three coated samples. Most of the particles are composed of a single coated hematite particle, having reasonably spherical core–shell units.

We measured the light scattering properties of the colloidal systems with a Malvern 4700 PCS spectrometer (Malvern Instruments). The light source used was a 75-mW argon-ion laser (Cyonics Model 2213, $\lambda_0 = 488$ nm, perpendicularly polarized). To avoid multiple scattering, the volume fraction of the suspensions was kept low ($\phi \leqslant 10^{-5}$).

A series of intensity measurements $i_e(\theta_k)$ were carried out at scattering angles 5° apart between 20° and 150°. Our approach was to calculate a number of theoretical intensities for these angles for a variety of core diameter, shell thickness, and polydispersity indices $i_e(\theta_k) = i_e(\theta_k, X, Y, \sigma_{0x}, \sigma_{0y})$ until a parameter set was found that best fit the experimental data. This was done by minimizing the error parameter:

$$\mathrm{ERR} = \frac{1}{N}\sum_{k=1}^{N}\left(1 - \frac{i_t(\theta_k)}{i_e(\theta_k)}\right)^2. \qquad [6]$$

To overcome the dependence of $i_e(\theta)$ upon other parameters (laser power, particle-detector distance, and particle concentration), all intensities were normalized to a common reference angle (60°), so that $i_t(\theta_0) = i_e(\theta_0) = 1$. Since a multiparameter fit could be multivalued and time-consuming, the indices of refraction were obtained from the literature. We used the values $n_0 = 1.3368$ for water (13), $n_1 = 1.65$ for yttrium basic carbonate (14), and $n_2 = 3.086 + i0.491$ for hematite (15, 16).

The number of remaining parameters was reduced from four to three by restricting the system to one of three choices: constant core radius, constant shell thickness, or constant thickness/core ratio. Earlier applications of this method have assumed a constant shell thickness, but electron micrographs taken before and after coating show clearly that this is not necessarily the case. Repeated tests based on experimental data and on theoretical runs have always showed this three-parameter approach to yield a unique solution, therefore ruling out the existence of multiple solutions to the inverse problem, even in the absence of maxima, minima, or other characteristic features of the $i-\theta$ curve.

The computer program was written in Fortran-77 to reproduce light scattering properties. All computations were carried out in a 9-processor Silicon Graphics Power Challenge mainframe at the University of Granada's computer service (the program can also be run on a personal computer).

RESULTS AND DISCUSSION

The Aden–Kerker theory was tested on three samples, labeled B_2, B_9, and D_9, which were synthesized from the same sized core material. The ZOLD size parameters for these coated samples, as well as those for the bare nucleus, are shown on Table 1. As seen, one of the samples (D_9) has a polydispersity similar to that of the nucleus, whereas systems B_2 and B_9 are considerably more polydisperse. Therefore, it makes sense to try to adjust the theoretical data under the constant core assumption for samples B_2 and B_9. On the other hand, the similarity in polydispersity between core and outer radius in sample D_9 suggests that a constant core–shell ratio approach would be more suit-

TABLE 1
Particle Size Distribution of Colloidal Suspensions as Determined by Electron Microscopy

Sample	d_m (nm)	σ_o
core	54 ± 10	0.17
B_2	78 ± 19	0.22
B_9	130 ± 44	0.29
D_9	167 ± 22	0.13

able. Theoretical fits yield the results given in Table 2, while experimental vs theoretical light scattering curves are shown in Figs. 4–6.

The most striking feature of these results is the large value of the calculated distribution width compared to that obtained by electron microscopy. This can be explained on theoretical grounds. For a perpendicularly polarized incident light source and a certain range in particle size (diameters under a few hundred nanometers), the calculated intensity curves lack characteristic features (maxima and minima) and show a monotonically decreasing trend with increasing angles. Increasing values of the polydispersity have relatively little effect (Fig. 7) on the angular intensity curves, due to this lack of peaks or other features. This limits the ability of our method to accurately determine polydispersity parameters. In general, polydispersity tends to smooth out characteristic features, and it affects results more strongly at higher values of the size parameter (see, e.g., Fig. 8). If measurement errors were small, this fact would have little influence on the results; however, experimental data are affected to some extent by three main causes: experimental errors, intensity averaging of repeated runs (to minimize sedimentation and aggregation effects), and the actual polydispersity of the system. With experimental errors on the order of 3%, and averaging errors in the vicinity of 5%, the computer program lacks accurate intensity data for the fit procedure. The curve is smoothed within a theoretical range, where these intensity curves are naturally featureless. The analysis trend favors a larger degree of polydispersity, resulting in a lower value of core thickness. A large value of σ_0 results in an increasing fraction of the larger particles, whose light scattering power is greater. The effect of nonsphericity must also be taken into account.

TABLE 2
Particle Size Distribution Data Obtained by Light Intensity Particle Sizing

Sample	Option	d (core, mn)	d_m (nm)	σ_o
B_2	Constant core	53	82	0.71
B_9	Constant core	58	80	0.77
D_9	Constant core/coat ratio	52	118	0.34

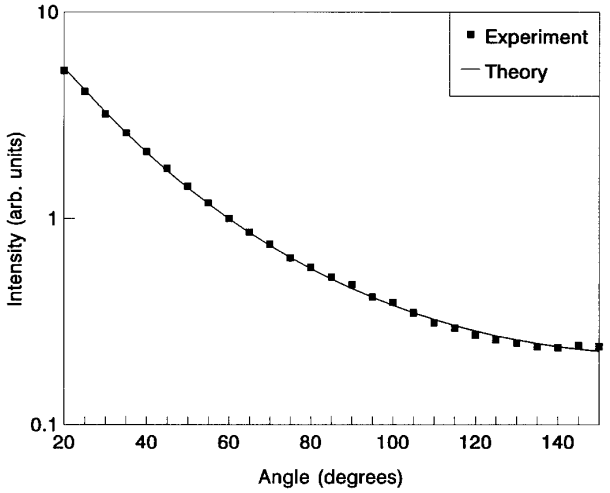

FIG. 4. Experimental and theoretical (Aden–Kerker) dependence of the intensity scattered by particle B_2.

Electron microscopy pictures suggest that a small number of particles have two nuclei and the resulting particle is rather nonspherical. Differences between experimental intensity and theoretical predictions based on EM data suggest a larger scattering power at large angles, in accordance with the general behavior found by other authors (see, e.g., Ref. 21).

On the other hand, a good core radius and (modal) shell thickness agreement is found on samples B_2 and B_9, where constant core conditions were assumed. Results on sample D_9 show good agreement in the determination of core radius, but fail to accurately determine core thickness. This is not surprising, since both core and coating have different degrees of polydispersity. The constant core assumption is inadequate for this analysis and would yield incorrect results: compared to data obtained under the constant core/shell ratio hypothesis, the shell modal radius barely changes, and the

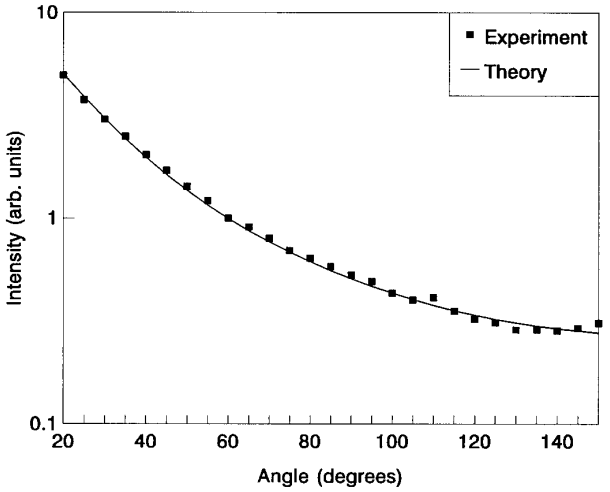

FIG. 5. Same as Fig. 4, for sample B_9.

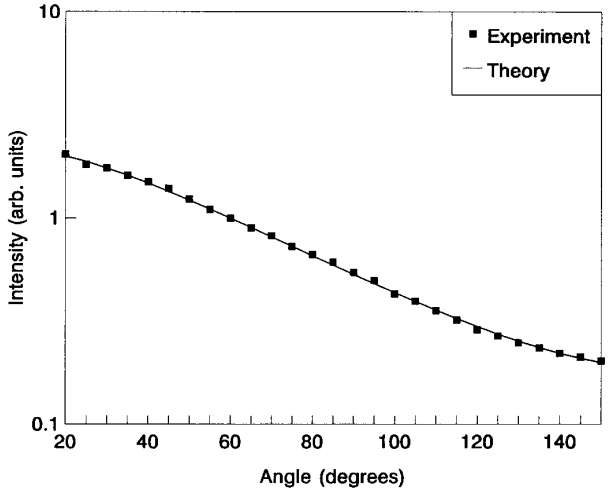

FIG. 6. Same as Fig. 4, for sample D_9.

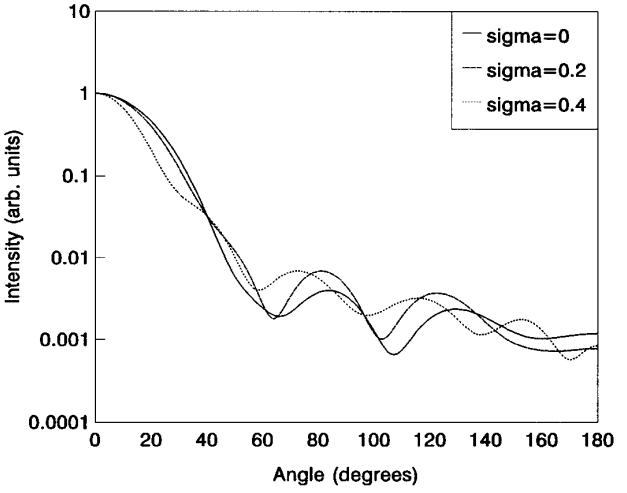

FIG. 8. Light scattering (Aden–Kerker theory) for coated particles with a hematite nucleus of constant radius, 200 nm, and a distribution of coating thickness with modal thickness $Z = 100$ nm and width $\sigma_0 = 0$, 0.2, and 0.4 (incident light, $\lambda_0 = 488$ nm, vertical polarization; suspending medium, water).

total diameter approaches electron microscopy data to within 1%, but the core radius shows an 88% increase.

This is an indication that any attempt to determine size distributions on polydisperse, coated spherical systems by light scattering techniques has to be based on a strong knowledge (or reasonable hypothesis) about the polydispersity assumed: whether of the core, the radius, or both. Previous applications of this theory were based on simplifying hypotheses such as Rayleigh scattering, effective refractive index, or the thin shell approximation (2, 17–20). In cases where monodispersity could not be assumed, an *a priori* polydispersity (constant core or constant core/shell ratio) value was assumed from electron microscopy data. Whereas some of these approximations are plausible in some systems (bubbles, very small particles, or carefully controlled syntheses), applications of the Aden–Kerker theory for particle sizing on real, polydisperse natural systems will require a careful choice of the value of polydispersity which is known (or assumed) to exist, along with a knowledge of the refractive indices for the particles (nucleus, coating, and surrounding medium).

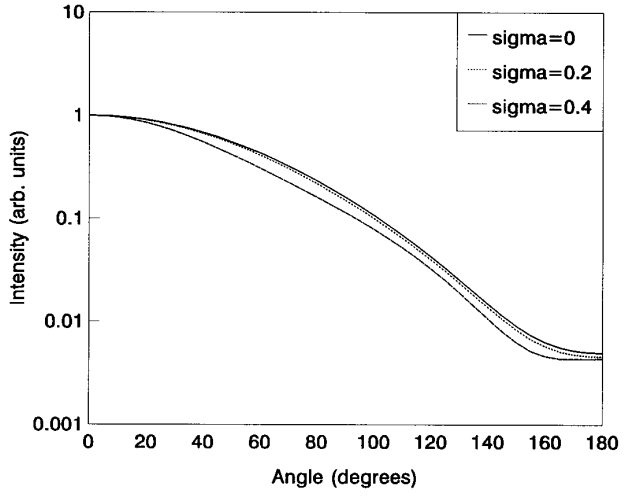

FIG. 7. Light scattering (Aden–Kerker theory) for coated particles with a hematite nucleus of constant radius, 80 nm, and a distribution of coating thickness with modal thickness $Z = 40$ nm and width $\sigma_0 = 0$, 0.2, and 0.4 (incident light, $\lambda_0 = 488$ nm, vertical polarization; suspending medium, water).

APPENDIX

The equations used in the calculation of the coefficients a_n and b_n do not follow the original Aden–Kerker formulation (7), but are closer to the Bohren and Huffman formalism (22). The coefficients a_n and b_n can be calculated as

$$a_n = \frac{(X_n/m_2 + n/y)\Psi_n(y) - \Psi_{n-1}(y)}{(X_n/m_2 + n/y)\xi_n(y) - \xi_{n-1}(y)} \qquad [7]$$

$$b_n = \frac{(Y_n m_2 + n/y)\Psi_n(y) - \Psi_{n-1}(y)}{(Y_n m_2 + n/y)\xi_n(y) - \xi_{n-1}(y)}, \qquad [8]$$

where

$$X_n = \frac{P_n(m_2 y)D_n(m_2 y) - A_n G_n(m_2 y)}{P_n(m_2 y) - A_n} \qquad [9]$$

$$Y_n = \frac{P_n(m_2 y)D_n(m_2 y) - B_n G_n(m_2 y)}{P_n(m_2 y) - B_n} \qquad [10]$$

and

$$A_n = P_n(m_2x)\,\frac{m_2D_n(m_1x) - m_1D_n(m_2x)}{m_2D_n(m_1x) - m_1G_n(m_2x)} \qquad [11]$$

$$B_n = P_n(m_2x)\,\frac{m_1D_n(m_1x) - m_2D_n(m_2x)}{m_1D_n(m_1x) - m_2G_n(m_2x)}, \qquad [12]$$

where

$$D_n(z) = \frac{\psi_n'(z)}{\psi_n(z)}, \quad G_n(z) = \frac{\chi_n'(z)}{\chi_n(z)},$$

$$P_n(z) = \frac{\psi_n(z)}{\chi_n(z)}, \qquad [13]$$

and $\psi_n(z) = z j_n(z)$, $\chi_n(z) = -z y_n(z)$, $\xi_n(z) = \psi_n(z) - \chi_n(z)$ are the Ricatti–Bessel functions (8). A time dependence of $\exp(-i\omega t)$ was assumed.

ACKNOWLEDGMENT

The financial support by DGICYT, Spain (Project PB94-0812-C02-1) is gratefully acknowledged.

REFERENCES

1. Mie, G., *Ann. d. Phys.* **25,** 377–445 (1908).
2. van Zante, J., and Monbouquette, G., *J. Colloid Interface Sci.* **146,** 330–336 (1991).
3. Wu, C., *Macromolecules* **27,** 7099–7102 (1994).
4. Strawbridge, K. B., and Hallett, F. R., *Can. J. Phys.* **70,** 401–406 (1992).
5. van Stavaren, H. J., Mose, C. J. M., van Marle, J., Prahl, S. A., and van Gemert, J. C., *Appl. Opt.* **30,** 4507–4514 (1991).
6. Meyer, R. A., *Appl. Opt.* **18,** 585–588 (1979).
7. Aden, A. L., and Kerker, M., *J. Appl. Phys.* **22,** 1242–1246 (1951).
8. Abramowitz, M., and Stegun, I. A., ''Handbook of Mathematical Functions.'' Dover, New York, 1972.
9. Espenscheid, W. F., Kerker, M., and Matijević, E., *J. Phys. Chem.* **68,** 3093–3097 (1964).
10. Matijević, E., and Scheiner, P., *J. Colloid Interface Sci.* **63,** 509–524 (1978).
11. Aiken, B., and Matijević, E., *J. Colloid Interface Sci.* **126,** 645–649 (1988).
12. Kawahashi, N., and Matijević, E., *J. Colloid Interface Sci.* **143,** 103–110 (1991).
13. Kerker, M., ''The Scattering of Light and Other Electromagnetic Radiation,'' Chap. 7, p. 324. Academic Press, New York, 1969.
14. Aiken, B., Hsu, E. P., and Matijević, E., *J. Am. Ceramic Soc.* **71,** 845–853 (1988).
15. Kerker, M., Scheiner, P., Cooke, D. D., and Kratohvil, J. P., *J. Colloid Interface Sci.* **71,** 176–187 (1979).
16. Hsu, W. P., and Matijević, E., *Appl. Opt.* **24,** 1623–1630 (1985).
17. Aragon, S. R., and Elwenspoek, M., *J. Chem. Phys.* **77,** 3406–3413 (1982).
18. Charalampopoulos, T. T., Hahn, D. W., and Chang, H., *Appl. Opt.* **31,** 6519–6528 (1992).
19. Hsu, W. P., Yu, R., and Matijević, E., *J. Colloid Interface Sci.* **156,** 56–65 (1993).
20. Philipse, A. P., Smits, C., and Vrij, A., *J. Colloid Interface Sci.* **129,** 335–352 (1989).
21. Wiscombe, W. J., and Mugnai, A., *Appl. Opt.* **27,** 2405–2421 (1988).
22. Bohren, C. F., and Huffman, D. R., ''Absorption and Scattering of Light by Small Particles.'' Wiley, New York, 1983.